Andreev tunneling enhanced by Coulomb oscillations in superconductor-semiconductor hybrid Ge/Si nanowire devices

Xiao-Jie Hao, Hai-Ou Li, Tao Tu, Cheng Zhou, Gang Cao, Guang-Can Guo, Guo-Ping Guo, Wayne Y. Fung, Zhongqing Ji, and Wei Lu

Phys. Rev. B **84**, 195448 — Published 21 November 2011

DOI: 10.1103/PhysRevB.84.195448

Andreev tunneling enhanced by Coulomb oscillations in superconductor-semiconductor hybrid Ge/Si nanowire devices

Xiao-Jie Hao[(1,2)], Hai-Ou Li[(1)], Tao Tu[(1)],* Cheng Zhou[(1)], Gang Cao[(1)], Guang-Can Guo[(1)], Guo-Ping Guo[(1)],† Wayne Y. Fung[(2)], Zhongqing Ji[(2)], and Wei Lu[(2)‡]

[(1)] *Key Laboratory of Quantum Information, University of Science and Technology of China, Chinese Academy of Sciences, Hefei 230026, People's Republic of China*

[(2)] *Department of Electrical Engineering and Computer Science, The University of Michigan, Ann Arbor, Michigan 48109, USA*

Abstract

We explore the magneto-conductance of Ge/Si core/shell nanowire quantum dot devices contacted by superconducting leads. Significant magneto-conductance peaks around zero field are observed and show a periodic modulation with gate voltage as discrete states of the quantum dot are turned on- and off-resonance with the Fermi energy in the superconducting electrodes. The ability to create and control coherent transport in superconductor-semiconductor hybrid nanostructures allows for new opportunities in the study of various fundamental competing effects such as superconductivity and electron-electron interactions.

The novel and fruitful electrical transport phenomena when low-dimensional conductors such as carbon nanotubes[1–9], semiconductor nanowires[10–14] or graphene[15–20] are connected to superconductors have attracted a lot of attentions in recent years. In these nanoscale devices, transport properties will highly depend on the interplay and competition of various mesoscopic effects in the superconducting electrodes and the nanostructures embedded between them. For a high transparency interface, the electronic transport exhibits Fabry-Perot interference in the normal state and will be strongly affected by the superconducting proximity effect, which can be evident from the observation of supercurrent and multiple Andreev reflections through the device[3,7,12,16]. For an intermediately transparency interface, the interactions between superconductivity and Kondo correlation can be observed[5,9,13]. For a low transparency interface, a quantum dot will be defined and the superconducting nature of the electrodes manifests itself through opening a gap in the Coulomb blockade regime[14]. It would be highly desirable to explore the last regime mentioned above which less attention has been paid to. In particular, in previous investigations, magneto-transport through the sample was typically not studied, whereas it has been proven as an essential signature for the underlying quantum coherent phenomena[21–23]. Here we report an extensive magneto-conductance measurement of Ge/Si core/shell nanowire quantum dots with superconducting leads, which provides a promising platform for the study of quantum coherent transport in combination with superconductivity[12]. We observe a remarkable peak in the magneto-conductance and dramatic oscillations periodic with the gate voltage when successive discrete energy levels in the nanostructure are tuned with respect to the Fermi energy in the superconducting leads. We attribute the enhanced peak to a Coulomb oscillation enhanced Andreev tunneling through the quantum dot, in sharp contrast to being suppressed as in previous studies[14].

The devices reported were fabricated on undoped Ge/Si core/shell nanowires grown by a two-step chemical vapor deposition[24]. Due to the large valence band offset between the Ge core and the Si shell, one-dimensional hole gas can be confined in the Ge channel. After growth, the nanowires were solution transferred to a heavily doped Si wafer with 50 nm silicon oxide, which was used as a back gate in the measurement. After locating the nanowires relative to the predefined markers on the substrate using scanning electron microscope (SEM), source and drain contacts were patterned by electron-beam lithography. To remove the native oxide outside the Si shell of the nanowires for good contact, the

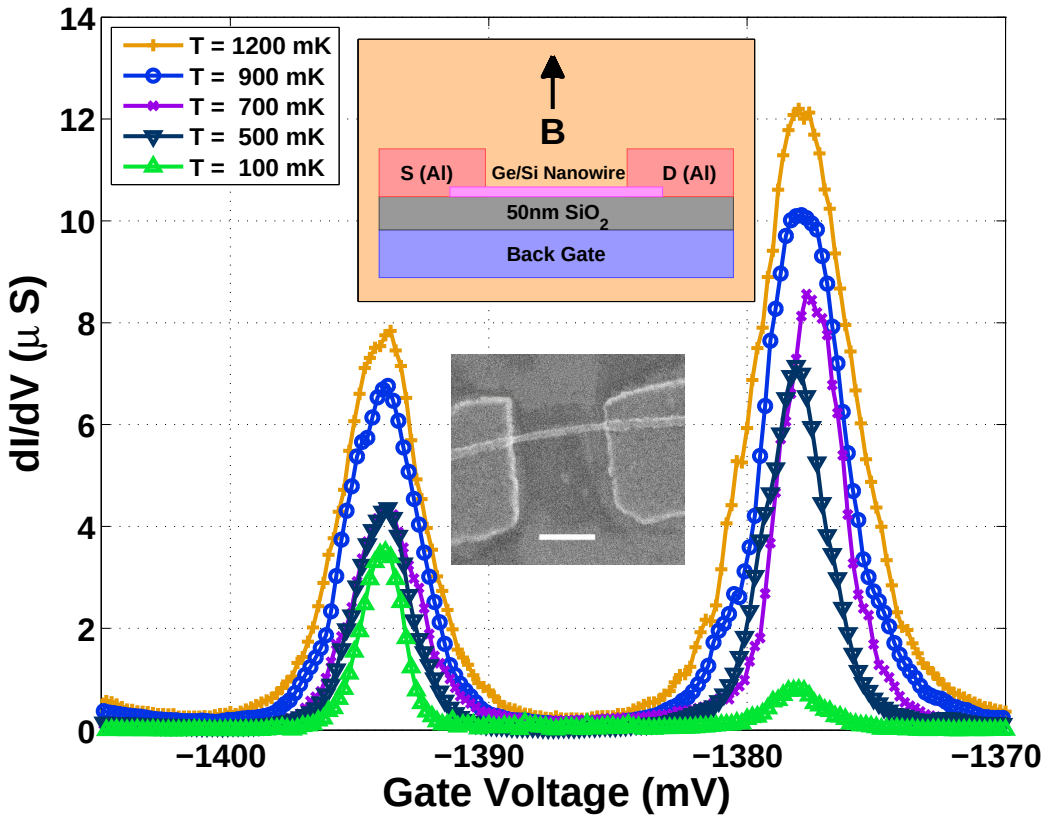

FIG. 1. (Color online) Temperature dependence of the differential conductance through the device as a function of back gate voltage at magnetic field $B = 60$ mT. (Upper inset) Experiment setup. (Lower inset) SEM image of one device (scale bar: 200 nm).

samples were immersed in buffered hydrofluoric acid for 3 seconds. Then 40 nm thickness of Aluminum (Al) electrodes were deposited. Nearly Ohmic contacts between the Al leads and the nanowires were obtained without annealing. SEM image of one of our devices is shown in the lower inset of Fig. 1.

The measurements were carried out in a top-loading dilution refrigerator with an environment base temperature of 20 mK. In the measurements, we employed the standard AC lock–in technique with an excitation voltage of 4 μV at 11.3 Hz. As shown in Fig. 1, we observe clear Coulomb blockade peaks at a wide range of V_g in the normal state, which demonstrates that the hole channel in the nanowires form a small quantum dot in the Coulomb blockade regime and the energy levels in the dot can be tuned by the gate voltage[25].

We then applied a magnetic field perpendicular to both the axis of the nanowire and the substrate (Upper inset of Fig. 1) and measured the magneto-conductance for a fixed V_g

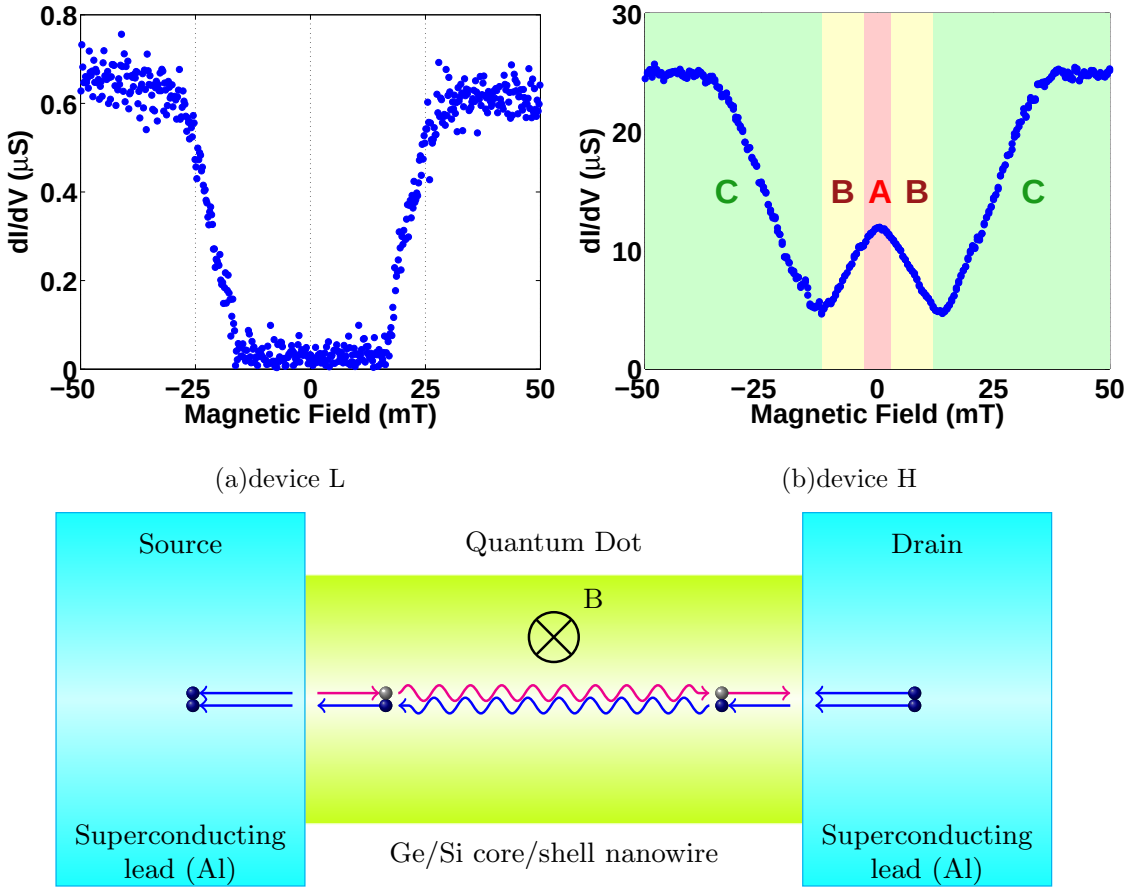

(a)device L (b)device H

(c)

FIG. 2. (Color online) Magneto-conductance for (a) the device L and (b) device H ($T = 50$ mK). (c) Schematic diagram of the Coulomb oscillation enhanced Andreev tunneling in the nanowire quantum dot. White open (Blue closed) dots denote electrons (holes).

corresponding to one of the Coulomb blockade oscillation peaks. Two devices, labeled as L and H, will be discussed here. First, a broad zero magneto-conductance dip with width of $2B_c$ is observed for device L in Fig. 2(a). Here $B_c \approx 15$ mT is the critical magnetic field to preserve Al electrodes in superconducting state. Second, the above kind of dip can still be observed from device H in Fig. 2(b). However in contrast to the device L case, a remarkable peak around zero magnetic field appears superimposed on the expected conductance dip. We note the suppression of current at low magnetic field observed in device L was consistent with previous studies on magneto-conductance phenomena in such nanostructures[14]. On the other hand, the current peak near zero magnetic field observed in device H has not been reported before. From the conductance values of Coulomb blockade

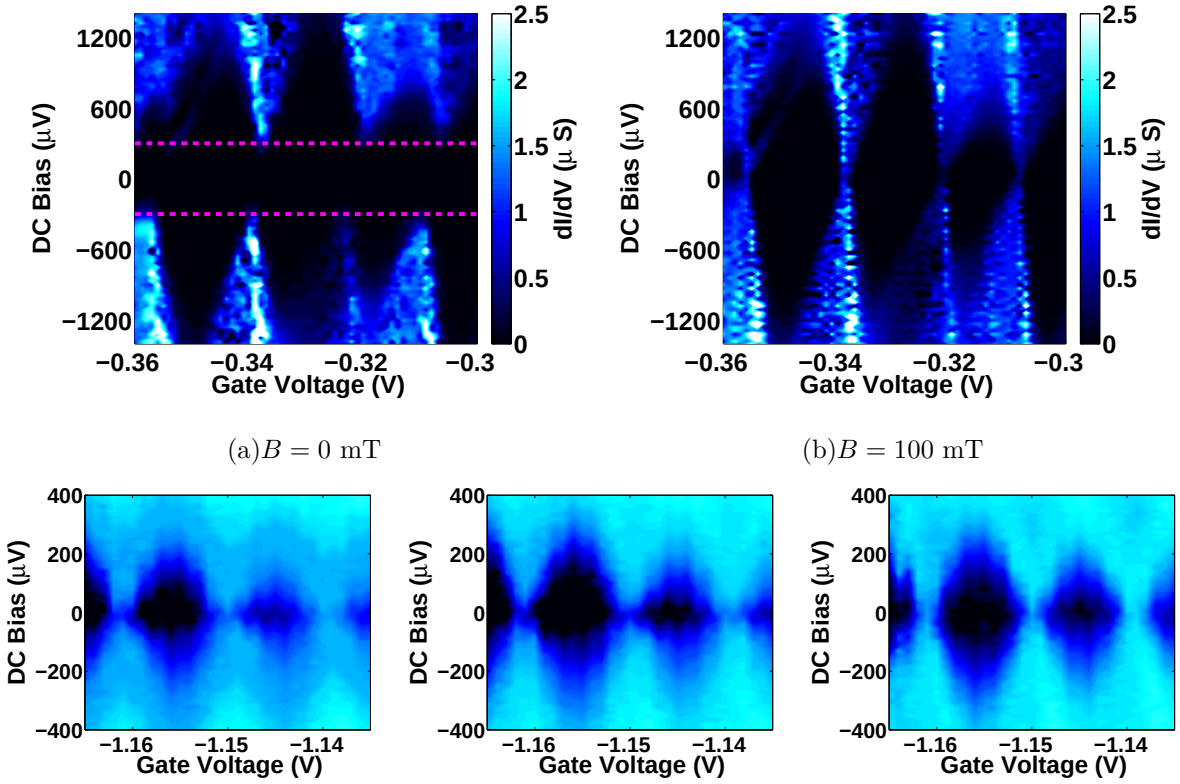

(a)$B = 0$ mT (b)$B = 100$ mT

(c)$B = 0$ mT (d)$B = 12$ mT (e)$B = 60$ mT

FIG. 3. (Color online) Stability diagrams for device L at (a) $B = 0$ mT and (b) $B = 100$ mT, and for device H at (c) $B = 0$ mT, (d) $B = 12$ mT, and (e) $B = 60$ mT with same color axis. All data were taken at $T = 50$ mK. The red dashed lines in (a) indicate the current suppression window due to the superconducting gap $2\Delta_{Al}$. In the light blue (dark black) regions, differential conductance dI/dV has large (small) values.

peaks in the normal state ($|B| > 40$ mT region in Fig. 2(b)), we estimate the tunneling rate between the source/drain lead and the quantum dot to be around 2.5 μeV (0.062 μeV) for the device H (L). That is, while the tunneling rates for both devices are smaller than the superconducting gap $2\Delta_{Al} \approx 300$ μeV, i.e. they are in the low transparency regime discussed earlier, the tunneling rate in device H is much higher than that in device L[26].

More information can be obtained from a measurement of the stability diagram with varying magnetic field. As shown in Fig. 3 for both devices, the differential conductance dI/dV is plotted as a function of DC source drain bias voltage $V_{SD(DC)}$ and gate voltage V_g at different magnetic fields. The light blue (dark black) regions in these figures represent large (small) values of differential conductance dI/dV. For device L, the current flow will be

blocked when the energy difference between the source and the drain is less than the quasi-particle superconducting gap $2\Delta_{Al}$. So in the stability diagram, currents are suppressed within a window of $4\Delta_{Al}/e$ (e is the element charge) at the cross point of two adjacent Coulomb diamonds, as indicated by the red dashed lines in Fig. 3(a). The current suppression can be lifted by the application of a magnetic field $B > B_c$, as illustrated in Fig. 3(b). All these observations are consistent with the previous studies[14]. On the other hand, for the device H it is obvious that the current suppression around zero bias is less pronounced even at $B = 0$ mT (Fig. 3(c)). A current suppression window starts to appear, however, as the magnetic field is increased, and reaches a maximum at $B = 12$ mT but the size of the suppression window is still significantly less than $4\Delta_{Al}/e$ (Fig. 3(d)). After $B > B_c$, this window vanishes as the Al leads collapses into the normal (non-superconducting) state (Fig. 3(e)).

The unusual magneto-conductance phenomena presented here for device H is clearly different from the ones reported before[14], which implies that a new transport mechanism exists in this system. Since the magneto-transport shows positive magneto-conductance at very low field, weak anti-localization could be one possible origination of the zero field peak. However, based on our previous investigation of weak anti-localization and spin-orbit coupling in this system[27], the enhancement of conductance could not be so strong for a change of several milliteslas in the magnetic field. Besides, as described below, this feature disappears at temperature T larger than the critical temperature of Al: $T_c \approx 1.2$ K, but weak anti-localization survives even as the temperature goes beyond 100 K. Here, we ascribe the unusual magneto-transport phenomena to a Coulomb oscillation enhanced Andreev tunneling through the quantum dot[3,6]. Briefly, the gate voltage tunes the energy levels in the nanowire quantum dot with respect to the Fermi energy in the superconducting leads. This discrete state provides an available channel for coupling the superconducting state in the leads. As shown in the Fig. 2(c), when one hole tunnels in the nanowire and incidents at the interface of the nanowire and the superconducting drain, it will be reflected as an electron in the nanowire and also destroys a Cooper pair in the drain due to Andreev reflection[28]. When this electron travels through the nanowire and incidents at the other interface between the nanowire and the superconducting source, it will be reflected as a hole and create a Cooper pair in the source. Since the phase coherence length for hole propagation in the nanowire is comparable to the distance between source and drain contacts[10,27], this process is phase

coherent which can be viewed as a consequence of the diffusion of Cooper pairs throughout the entire length of the nanowire between the two superconducting electrodes[11]. Within this picture, one may gain at least a qualitative understanding of the features observed in the magneto-conductance measurement. For example, in Fig. 2(b) there are three distinct regions labeled as 'A', 'B' and 'C'. In region 'A', even if there are superconducting gaps in the source and drain leads, the current can still flow through the device at zero bias due to Andreev reflection assisted phase coherent tunneling discussed above, leading to an enhancement in the conductance below the superconducting gap. While in region 'B' an external magnetic field less than B_c applied perpendicular to the transport path will break the phase information during the transport. That causes the phase coherent transport to be suppressed and results in a decrease of the differential conductance with increasing magnetic field. In region 'C' a larger magnetic field exceeding the critical field B_c destroys the superconducting state in electrodes so the transport falls to the usual Coulomb blockade oscillation regime and the conductance recovers to the normal value.

An interesting aspect of this magneto-transport is that it can be strongly modulated by means of a gate voltage, as shown in the false-color plot of Fig. 4. We find that the pronounced magneto-conductance feature follows a periodic modulation and can be turned on or off by the gate voltage. Only if an energy level in the quantum dot is aligned with the Fermi levels of the source and the drain (indicated as light blue lines in Fig. 4 and 'ON' state in the left inset of Fig. 4), a channel could open for the Andreev reflections at the interfaces of nanowire and Al, therefore the transport could happen. Otherwise, the transport is dramatically suppressed (indicated as dark black regions in Fig. 4 and 'OFF' state in the right inset of Fig. 4). Moreover, it is obvious that the strength of the zero-field magneto-conductance peak depends on the Coulomb oscillation in the normal state. This is consistent with the picture that the probability of the Andreev reflection depends on the effective transparency of the interface, i.e. the overlap of energy levels in the quantum dot with Fermi levels in the source and drain electrodes[3,6]. This gate tunable phenomenon is similar to a supercurrent transistor in carbon nanotubes reported by Jarillo-Herrero *et al.*[3]. In their experiments, the supercurrent and multiple Andreev reflections can be turned on and off by gating the carbon nanotube at different Febry-Perot interference regions. Notably, the normal state conductance in the region where the supercurrent was observed in their device is slightly higher than ours but in the same order of e^2/h (h is the Planck's constant).

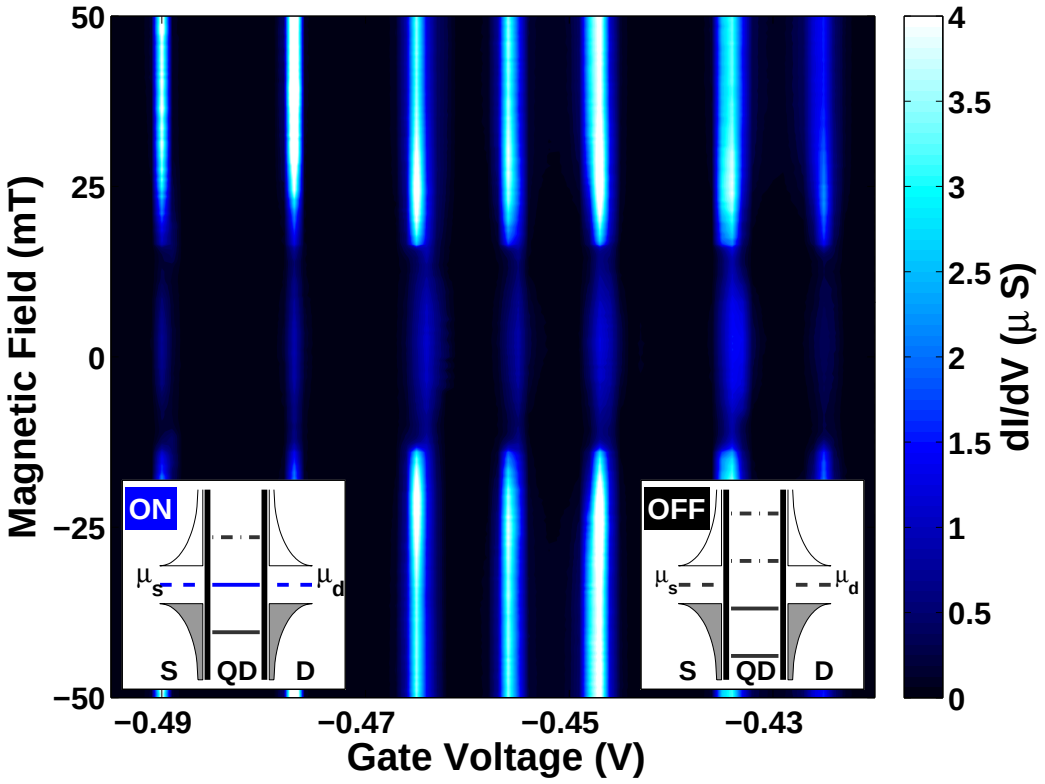

FIG. 4. (Color online) Color-scale plots of the differential conductance as a function of the magnetic field and the back gate voltage at $T = 50$ mK and zero DC bias. (left inset) Schematic diagram of the 'ON' state, in which an energy level is aligned to the Fermi energies of the superconducting leads and the Andreev tunneling occur between the leads. (right inset) Schematic diagram of the 'OFF' state, in which the current flow is turned off by means of gate voltage.

The key factor which is responsible for the Andreev tunneling in our system is the interface transparency. The interface in device H is still resistive enough to allow the formation of a quantum dot in the Coulomb blockade regime but also transparent enough to allow the Andreev reflection processes. Therefore, in our case the gate voltage tunes the position of the energy levels of the dot and opens a channel at the position where the Andreev tunneling is enhanced by Coulomb oscillations. We emphasize that both superconductivity[3] and the magneto-transport as we show here exhibit a series of on- and off-resonance modulations with gate voltage and demonstrate the interplay between different types of electron-electron correlations such as superconductivity and Coulomb interactions. We also note that two basic parameters such as interface scattering and the interaction strength in the normal region are required to provide a qualitatively understanding of the observed new effect[29]. In

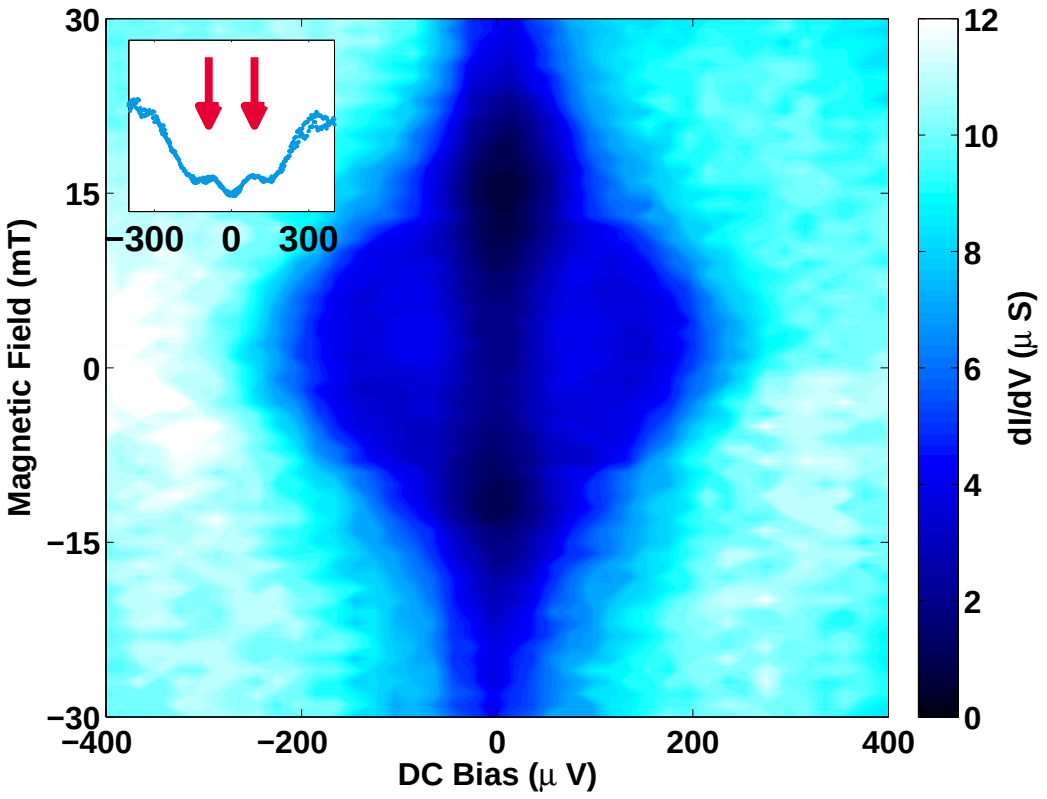

FIG. 5. (Color online) Color-scale plots of differential conductance as a function of magnetic field and DC bias voltage. Data were taken at $T = 50$ mK while fixing V_g at one of the Coulomb oscillation peaks. (inset: Differential conductance as a function of DC bias voltage at zero magnetic field.)

order to quantitatively understand the experimental results such as the peak amplitudes and their line shape shown in this work, more modeling parameters and a detailed theoretical calculation are needed.

Further support of the above interpretation is provided by additional data. In Fig. 5, the differential conductance dI/dV is plotted against the magnetic field B and the DC bias voltage $V_{SD(DC)}$ for a fixed V_g corresponding to one of the Coulomb blockade oscillation peaks. In this diagram, it is clearly seen that for $\left|V_{SD(DC)}\right| < 2\Delta_{Al}/e$, dI/dV has a local maximum at zero field and decreases as B increases, then goes up and saturates after $|B| > B_c$. This feature is not strictly restricted to the zero-bias condition and still be observed for non-zero bias voltages $\left|V_{SD(DC)}\right| < 2\Delta_{Al}/e$ owing to transport via Andreev tunneling through the excited states. The temperature dependence of the Coulomb blockade

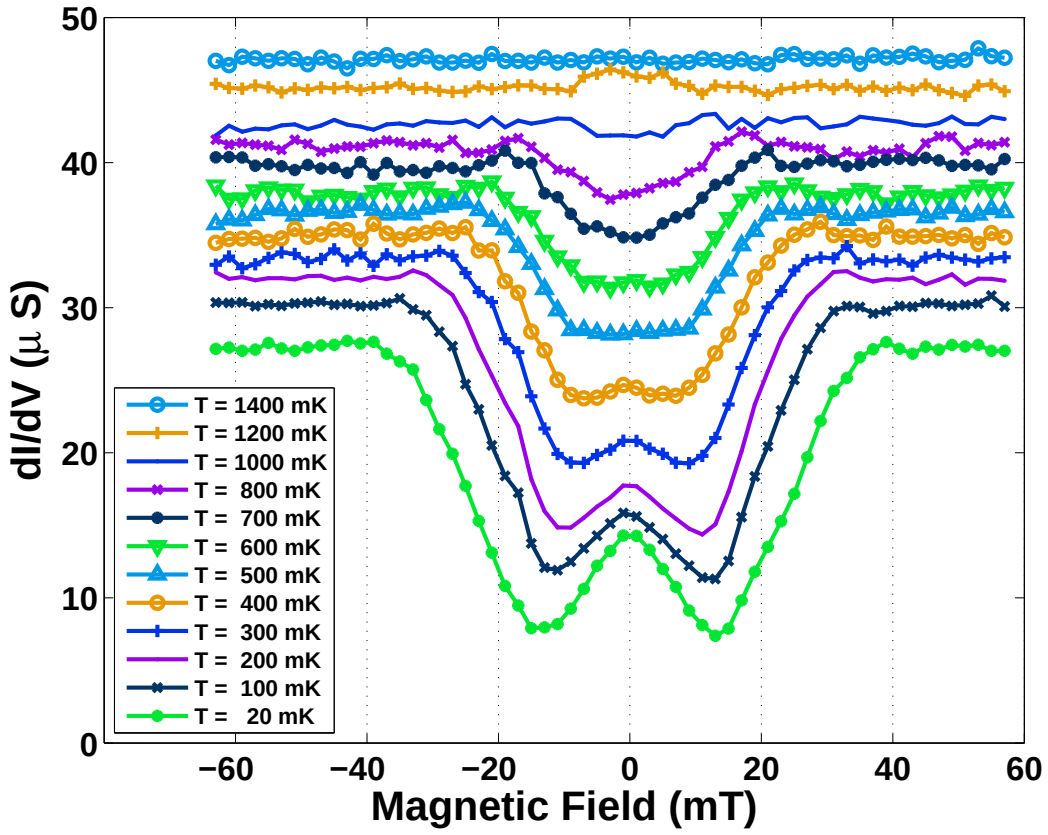

FIG. 6. (Color online) Plot of magnetic field dependent differential conductances at various of temperatures. The curves from top to down are taken at $T = 1400$, 1200, 1000, 800, 700, 600, 500, 400, 300, 200, 100, 20 mK, and are vertically shifted for clarity.

oscillations shown in Fig. 1 implies the energy level splitting in the quantum dot is much smaller than $K_B T$, where K_B is Boltzmann's constant and T is the temperature of charge carriers. It means that the dot we measured is in the classical Coulomb blockade regime, where many levels are excited by thermal fluctuations[30]. Moreover, as shown in the light blue regions in Fig. 3, the observation that the differential conductance keeps increasing while $V_{SD(DC)}$ increases also indicates tunneling through excited states through the quantum dot. There are also two faint plateau at $\left|V_{SD(DC)}\right| = 2\Delta_{Al}/2e = 150$ μV and $|B| < B_c$ (indicated by two arrows in the inset of Fig. 5), which correspond to the $n = 2$ multiple Andreev scattering[31].

We also tested the device at different temperatures. From the data given in Fig. 6, we find that the conductance dip due to the superconducting gap collapses and finally disappears at $T > T_c \approx 1.2$ K. On the other hand, the Coulomb oscillation enhanced

Andreev tunneling feature around zero magnetic field vanishes at a much lower temperature around $T = 500$ mK, at which temperature the superconducting gap in Al starts to decrease dramatically according to the superconductivity theory[32], and does not show up after $T > T_c$[33]. These observations confirm that the phase coherent transport is directly correlated to the superconducting states in the electrodes and is much easier to be destroyed by heating effect than the superconducting state in Al.

In conclusion, we observed an unusual magneto-conductance peak and its modulation with gate voltage corresponding to successive Coulomb blockade oscillations in superconductor-semiconductor hybrid quantum dot devices based on Ge/Si core/shell nanowires. We attributed the experimental phenomena to a Coulomb oscillation enhanced Andreev tunneling through the quantum dot, which is also phase coherent and can be suppressed by an external magnetic field. We end by noting that Ge/Si nanowires provide a potential convenient system for design of complex hybrid nanostructures, and further investigations are highly desired to explore the properties involving various competing effects such as superconductivity and electron-electron interactions.

This work was supported by the National Basic Research Program of China (Grants No. 2011CBA00200), the National Natural Science Foundation of China (Grants No. 10804104, No. 10874163, No. 10934006, No. 11074243), and the US National Science Foundation (ECS-0601478).

---

* tutao@ustc.edu.cn

† gpguo@ustc.edu.cn

‡ wluee@eecs.umich.edu

[1] A. Y. Kasumov *et al.*, Science **284**, 1508 (1999).

[2] A. F. Morpurgo *et al.*, Science **286**, 263 (1999).

[3] P. Jarillo-Herrero *et al.*, Nature **439**, 953 (2006).

[4] J.-P. Cleuziou *et al.*, Nature Nanotech. **1**, 53 (2006).

[5] M. R. Buitelaar *et al.*, Phys. Rev. Lett. **89**, 256801 (2002).

[6] M. R. Buitelaar *et al.*, Phys. Rev. Lett. **91**, 057005 (2003).

[7] H. I. Jørgensen *et al.*, Phys. Rev. Lett. **96**, 207003 (2006).

[8] J.-P. Cleuziou *et al.*, Phys. Rev. Lett. **99**, 117001 (2007).

[9] A. Eichler *et al.*, Phys. Rev. Lett. **99**, 126602 (2007).

[10] Y.-J. Doh *et al.*, Science **309**, 272 (2005).

[11] J. A. van Dam *et al.*, Nature **442**, 667 (2006).

[12] J. Xiang *et al.*, Nature Nanotech. **1**, 208 (2006).

[13] T. Sand-Jespersen *et al.*, Phys. Rev. Lett. **99**, 126603 (2007).

[14] Y.-J. Doh *et al.*, Nano Lett. **8**, 4098 (2008).

[15] H. B. Heersche *et al.*, Nature **446**, 56 (2007).

[16] F. Miao *et al.*, Science **317**, 1530 (2007).

[17] A. Shailos *et al.*, Europhys. Lett. **79**, 57008 (2007).

[18] X. Du *et al.*, Phys. Rev. B **77**, 184507 (2008).

[19] C. Ojeda-Aristizabal *et al.*, Phys. Rev. B **79**, 165436 (2009).

[20] B. M. Kessler *et al.*, Phys. Rev. Lett. **104**, 047001 (2010).

[21] P. W. Brouwer *et al.*, Phys. Rev. B **54**, R12705 (1996).

[22] A. A. Clerk *et al.*, Phys. Rev. B **62**, 10226 (2000).

[23] R. S. Whitney *et al.*, Phys. Rev. Lett. **103**, 247002 (2009).

[24] W. Lu *et al.*, Proc. Natl. Acad. Sci. U. S. A. **102**, 10046 (2005).

[25] See Supplemental Material at [URL will be inserted by publisher] for the estimation of the size of the dot and numbers of holes in the dot.

[26] See Supplemental Material at [URL will be inserted by publisher] for a detailed estimation of the tunneling rate.

[27] X.-J. Hao *et al.*, Nano Lett. **10**, 2956 (2010).

[28] A. F. Andreev, Sov. Phys. JETP **19**, 1228 (1964).

[29] O. T. Valls *et al.*, Phys. Rev. B **82**, 134534 (2010).

[30] L. P. Kouwenhoven *et al.* eds., *Electron Transport in Quantum Dots* (NATO ASI Conference Proceedings, Klewer, 1997).

[31] A. W. Kleinsasser *et al.*, Phys. Rev. Lett. **72**, 1738 (1994).

[32] M. Tinkham, *Introduction to Superconductivity* (McGraw-Hill, New York, 1996), ed. 2 edition.

[33] M. Octavio *et al.*, Phys. Rev. B **27**, 6739 (1983).